Research Square

Preprints are preliminary reports that have not undergone peer review.
They should not be considered conclusive, used to inform clinical practice,
or referenced by the media as validated information.

Using Locally Developed Allometric Equations Improves Biomass Estimation in Managed Forests

Amanda Schoonmaker
Northern Alberta Institute of Technology Center for Boreal Research
Angeline Dongen
Northern Forestry Center, Natural Resources Canada
Dani Degenhardt
dani.degenhardt@nrcan-rncan.gc.ca

Northern Forestry Center, Natural Resources Canada

Research Article

Keywords: Pre-commercial Thinning, Lodgepole Pine, National Allometric Equations, Biomass

Posted Date: September 24th, 2026

DOI: https://doi.org/10.21203/rs.3.rs-10934366/v1

License: This work is licensed under a Creative Commons Attribution 4.0 International License.
Read Full License

Additional Declarations: No competing interests reported.

Using Locally Developed Allometric Equations Improves Biomass Estimation in Managed Forests

Amanda Schoonmaker[a], Angeline Van Dongen[b], Dani Degenhardt[b]

[a] Northern Alberta Institute of Technology Center for Boreal Research. 8102 99 Avenue, Peace River, Alberta, Canada.

[b] Northern Forestry Center, Canadian Forest Service, Natural Resources Canada. 5320 122 Street NW, Edmonton, Alberta, Canada.

Corresponding author: dani.degenhardt@nrcan-rncan.gc.ca

Keywords: Pre-commercial Thinning, Lodgepole Pine, National Allometric Equations, Biomass

Key Message: Locally developed allometric equations that incorporate live crown attributes better predict biomass in pre-commercially thinned forests than national equations.

Abstract

Forest biomass allometric equations are widely used to quantify productivity, carbon stocks, and canopy fuels; however, generalized equations may not accurately reflect biomass allocation in intensively managed stands. This study evaluated the performance of locally developed versus national equations for predicting crown biomass in lodgepole pine (*Pinus contorta* var. *latifolia* Dougl.) stands subjected to pre-commercial thinning (PCT) in Alberta, Canada. Destructive sampling was conducted on 52 trees across nine replicated PCT sites, seven to eight years following thinning. Branch-level biomass models were developed for large branch, small branch, and foliage biomass using generalized linear mixed-effects models and subsequently scaled to whole-tree biomass equations. Diameter at breast height (DBH), height, and live crown percentage were identified as the strongest predictors of crown biomass. Locally derived equations produced strong model fits and demonstrated that trees in PCT stands had greater foliage and branch biomass than trees of similar DBH in untreated stands, with larger differences observed at larger DBHs. At the individual-tree level, the national and local equations were similarly correlated with observed foliage and branch biomass in both unmanaged and thinned stands. At the stand level, the national equations produced biomass estimates comparable to the local equations in unmanaged stands but significantly underestimated foliage and branch biomass in stands that had received PCT. Our findings indicate that generalized allometric equations may not adequately capture crown structural change associated with PCT treatments. The development of locally calibrated equations or site-specific adjustment factors may therefore improve biomass estimation in managed stands.

1. Introduction

Estimating forest biomass is fundamental to sustainable forest management and is essential for quantifying forest productivity (Bernier et al. 1999), carbon stocks (Kurz et al. 2013), and canopy fuel loads (Alexander and Cruz 2014). Biomass estimation is typically conducted at the individual tree level and subsequently aggregated to the plot level before being scaled to an area basis (Fournier et al. 2003). Direct determination of tree biomass is time-consuming and impractical, as it requires destructive sampling, including the separation and weighing of different tree components. Consequently, biomass is commonly estimated indirectly using allometric equations derived from empirical relationships between biomass components and more readily measured tree attributes. These equations are developed by fitting statistical models to sampled datasets to describe relationships between biomass components and variables such as diameter at breast height (DBH) and tree height (Jenkins et al. 2003).

Generalized allometric equations are often developed from pooled datasets collected across broad geographic regions. In Canada, national-scale allometric equations are widely used to estimate tree-level biomass components, including foliage, branches, stem bark, and stem wood, based on a dataset comprising thousands of trees across ten species (Lambert et al. 2005; Ung et al. 2008). These equations are considered generalizable because they are well suited for broad-scale biomass estimation (Jenkins et al. 2003). These national equations are appropriate for policy-related purposes such as carbon accounting and were selected as the preferred equations for developing Canada-wide area-based volume-to-biomass conversion models (Boudewyn et al. 2007).

Despite their broad applicability, generalized allometric equations may not accurately represent biomass relationships under specific site conditions or forest management practices.

Because these equations reflect average relationships across large datasets, many of which originated from unmanaged stands, their accuracy may decline when applied to local conditions (Hall and Richardson 2001; Ung et al. 2008). Case and Hall (2008) demonstrated that biomass prediction error increased with increasing levels of equation generalization when comparing local, regional, and national models. Xing et al. (2019) developed species-specific biomass equations for boreal tree species in northern Alberta using destructive sampling and found that national equations underestimated biomass for white spruce while overestimating biomass for aspen and balsam poplar. These discrepancies were attributed to local variation in biomass relationships resulting from intraspecific geographic differences. Fradette et al. (2021) also reported that national equations underestimated branch biomass for black spruce and jack pine in open woodlands of eastern Canada, likely because generalized equations did not account for crown structural differences associated with greater light intensity of open woodlands.

Forest density management practices such as pre-commercial thinning (PCT) and commercial thinning (CT) are often implemented with the goal of reducing rotation lengths and filling timber supply gaps as trees can reach merchantable size sooner (Baah-Acheamfour et al. 2023; Bhandari et al. 2024; Scaria and Pinno 2024). PCT is typically applied in young stands before trees reach merchantable size and involves the selective removal of competing stems to reduce stand density and improve growth of residual trees (Pitt and Lanteigne 2008; Gupta et al. 2020; Scaria and Pinno 2024). In contrast, CT is generally conducted in planted or managed stands where removed trees have merchantable value, with the objective of improving individual tree growth, stand quality, and future merchantable yield (Zeide 2001; Thiffault et al. 2011). Both treatments modify competition and light availability, leading to changes in stem form and crown morphology. Variations in crown morphology can further contribute to substantial

differences in branch and foliage biomass partitioning (Pulkkinen 1991). The application of generalized biomass allometric equations in these managed systems may lead to underestimation of biomass in thinned stands and overestimation in densely stocked stands with high competition; however, no study has directly evaluated the effect of PCT on lodgepole pine crown biomass and allometric relationships. Accordingly, the objective of this study was to evaluate the influence of localized versus generalized allometric equations for predicting crown biomass in density managed stands. Specifically, we quantified the effects of locally developed equations on estimates of branch and foliage biomass for lodgepole pine (*Pinus contorta* var. *latifolia* Dougl.) and compared these predictions with those derived from generalized national equations in stands that had received PCT treatment seven to eight years prior as well as in a paired set of stands where no PCT occurred, under conditions more reflective of the natural successional process in fire-origin pine stands.

2. Methods

2.1 Study area

The study area is located near Whitecourt, AB, Canada (Figure 1) within the foothills natural region and is dominated by mixedwood forests of aspen, lodgepole pine, and white spruce at lower elevations and lodgepole pine forests at higher elevations (Natural Regions Committee 2006). Mean monthly temperatures in the foothills region range from -12.8 ºC to 14.7 ºC and elevation ranges from 650 to 1750 m above sea level (Natural Regions Committee 2006).

The study area included nine study sites within an ongoing lodgepole pine pre-commercial thinning trial. The trial contains a series of replicated site installations with different levels of PCT. These sites were harvested between 1996 and 2010, originating from clearcuts and in some

cases the stands had burned prior to logging (fire-salvage). Following harvest, site preparation involved either drag scarification, no site preparation, or were planted (Table 1). The nine sites sampled in this study received PCT between 2018 and 2019 and were 8 to 22 years at the time of thinning and 15-29 years old at the time of tree sampling (Table 1).

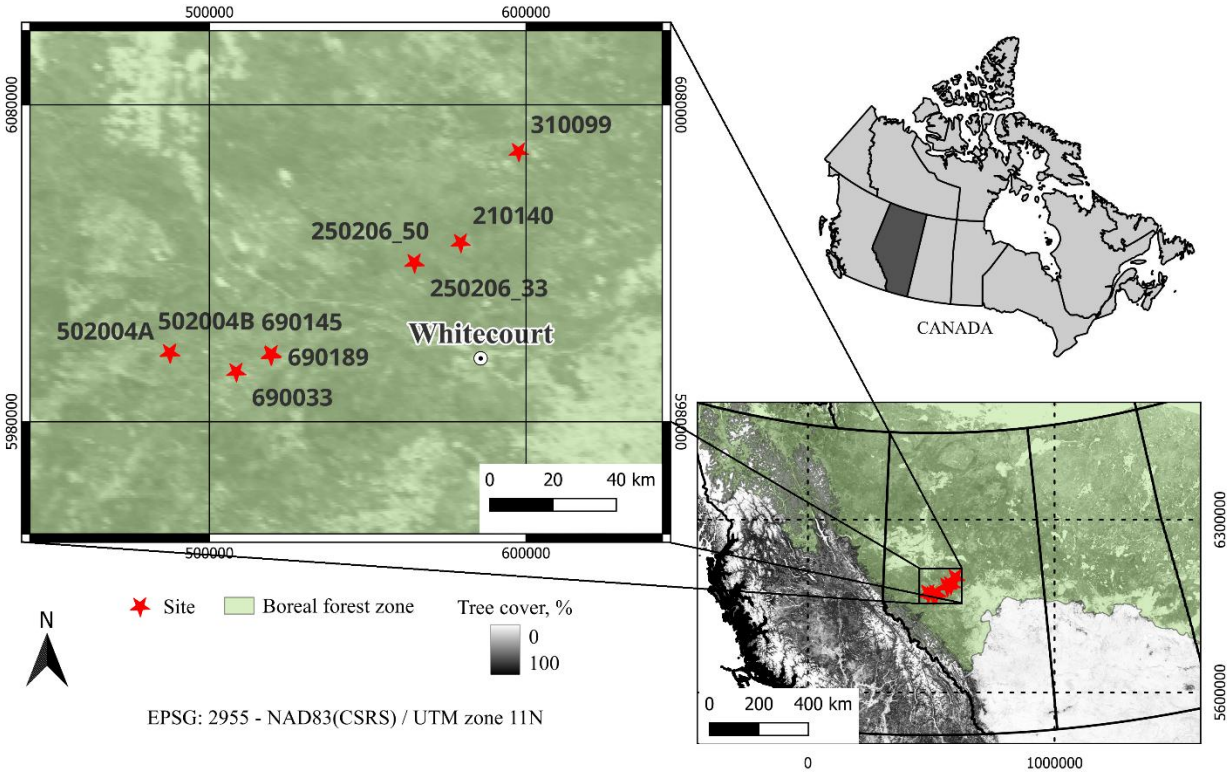


Figure 1. Study area near Whitecourt, Alberta, Canada. Stars indicate the nine study locations; note that stars appear to be overlapping for sites 502004A/502004B, 690145/690189 and 250206_33/250206_50 at this scale.

Table 1. Site characteristics including harvest year, origin, initial treatment, year of thinning, age at the time of thinning, and density at the time of sampling (7-8 years post thinning) of the

control (C) and thinned (T1, T2, and T3) plots. Salvage logged sites had burned prior to harvesting operations.

Site ID	Harvest Year	Origin	Initial treatment	Year of thinning	Age at thinning	Density at time of sampling (stems ha^{-1})			
						C	T1	T2	T3
210140	1996	clearcut	drag scarification	2019	22	9,556	1,600	2,311	2,667
250206_33	1998	salvage logged	no treatment	2019	20	24,000	1,733	4,089	3,733
250206_50	1998	salvage logged	no treatment	2019	20	25,733	2,667	3,911	2,978
310099	2005	clearcut	drag scarification	2018	12	8,400	2,622	3,200	4,622
502004A	2005	clearcut	drag scarification	2018	12	10,356	4,400	4,889	4,844
502004B	2005	clearcut	drag scarification	2018	12	12,889	5,022	4,400	7,733
690033	1996	clearcut	planted	2019	22	3,911	1,644	NA	NA
690145	2004	clearcut	drag scarification	2018	13	11,156	2,667	4,489	4,089
690189	2010	clearcut	drag scarification	2019	8	21,778	6,311	7,111	5,556

2.2 Experimental design

At each study site, a 70 × 70 m plot was installed in a location selected by random distance and random bearing. The plot location was visually assessed to confirm that the area was similar throughout and reflected stand conditions appropriate for PCT with brush saws. If a significant portion of the plot fell on an area that did not meet these criteria, the plot was moved to a suitable adjacent area.

Within each 70 × 70 m plot, one of four thinning prescriptions were assigned to a 35 × 35 m subplot (Figure A1). The sub-plot treatments included a control (no thinning) and three levels of planned thinning: once, twice, and three times over the stand rotation. The thinning treatments initially applied included: T1 (thinned to ~1,300 stems ha^{-1}), T2 (thinned to ~2,000 stems ha^{-1} with a future second thinning planned), and T3 (thinned to ~3,100 stems ha^{-1} with two future thinnings planned). The untreated control subplot (C) was always located in the NW corner, subplot T1 in the NE corner, subplot T2 in the SE corner, and subplot T3 in the SW corner (Figure A1). At one site (690033), only the C and T1 plots were established due to the initial stand densities being lower than the other sites.

At the time of biomass sampling, only the first intended thinning (PCT) was completed on the trial subplots in the spring of either 2018 or 2019. Pre-treatment and immediately post-treatment tree measurements were taken to characterize subplot to subplot variability (Table B1). The percent basal area removed at the time of thinning was between 22 and 71% depending on the site and subplot (Table B1). Biomass sampling occurred at each site in the summer of 2025, which was seven or eight years post-thinning. Plot densities at the time of sampling ranged from 3,911 to 25,733 stems ha^{-1} in the control plots and 1,600 to 7,733 stems ha^{-1} in the T1, T2, and T3 plots, herein referred to as thinned plots (Table B2).

2.3 Field measurements and tree harvest

Within each treatment subplot, a central 15 m x 15 m measurement plot was established and the species, status, height, DBH, height to live crown, and crown width of all trees within the measurement plot were recorded.

At each of the study site installations, six trees were selected for destructive harvest: three from the control plot and one from each thinned plot. For the T1, T2, and T3 plots, the tree

nearest but outside the SW corner, NW corner, and NE corner, respectively, of the measurement plot was tagged for harvest (Figure A1). For the control plot, two trees nearest, but outside the NW corner of the measurement subplot and one tree nearest, but outside the SW corner of the assessment subplot were tagged for harvest (Figure A1). In early July 2025, these tagged trees were felled with a chainsaw, and the following tree-level information was recorded: total height, height to live crown, DBH, and crown width. A total of 52 trees were felled across the nine sites: 27 from control plots and 25 from the thinned plots (Table 2).

Table 2. Descriptive characteristics of trees that were harvested. SD = one standard deviation of the mean.

Treatment	n	Parameter	Height (m)	DBH (cm)	Live crown (%)
Control	27	Mean (SD)	7.9 (2.8)	8.0 (3.4)	58 (15)
		Range	4.7-14.0	4.5-16.2	36-82
Thinned	25	Mean (SD)	7.8 (2.2)	10.1 (3.4)	71 (12)
		Range	4.8-12.8	5.7-18.8	47-90

2.4 Field sampling and lab processing of branches

The length, and diameter at the base of every living and dead branch on harvested trees were recorded in one-meter intervals along the stem. Across the 52 trees sampled, 4,185 live branches and 2,248 dead branches were measured. From each one-meter section where live branches were found, three branches were sub-sampled for determination of biomass pools.

These branches are henceforth referred to as primary branches as they originated from the stem and carried different biomass components: foliage, small branch and large branch mass. A total of 898 primary branches were sub-sampled for biomass determination across 52 overstory trees, representing 14% of the total number of branches.

The subsampled primary branches were dried in a drying room at 60ºC over a one-week period until a constant weight was observed. Following drying, each primary branch was manually separated into three biomass pools: foliage, small branches (< 0.5 cm diameter) and large branches (> 0.5 cm diameter) (Figure 2). The small branch size class was distinguished from the large branch size class for utility in canopy fuel modeling where canopy fuel is generally assumed to include both foliage and a small diameter fraction of the branchwood (Reinhardt et al. 2006). These components were then weighed to the nearest one gram.

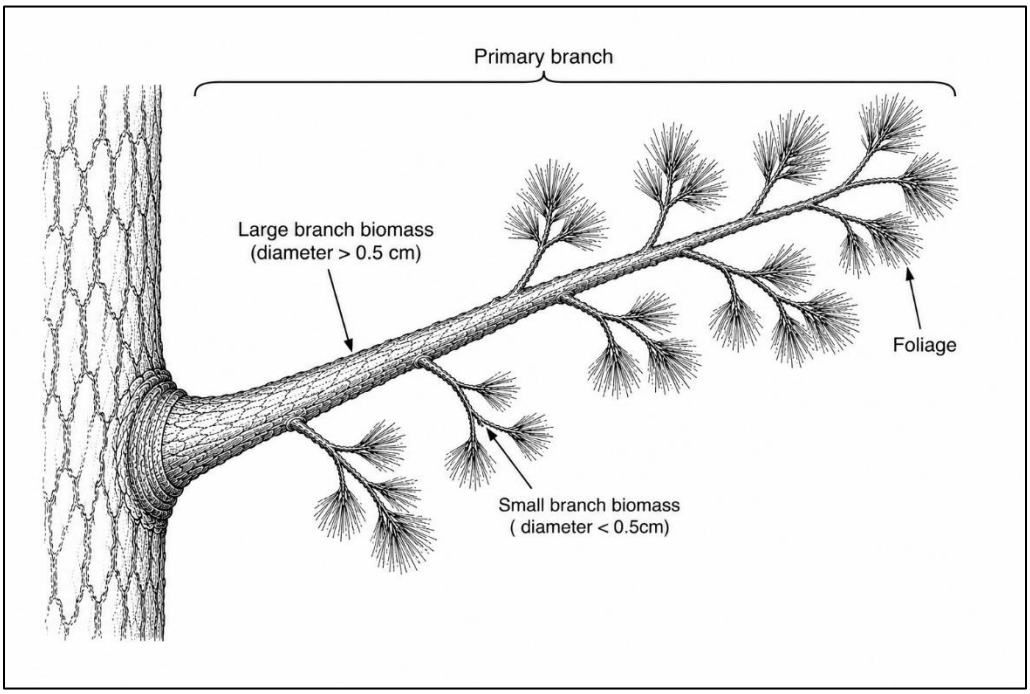


Figure 2. Schematic showing a primary branch with its three biomass pools: large branch biomass (diameter > 0.5 cm), small branch biomass (diameter < 0.5 cm), and foliage. Figure created using Claude.

2.5 Statistical approach used for model development

Data were analyzed using R statistical software (R Core Team 2025). Generalized linear mixed-effects models (GLMM) were employed and fitted using the function *glmmTMB* in the R package glmmTMB (Brooks et al. 2017). The distribution utilized for each response variable was modified based on the structure and best fit solution for each model. Nested random effects were included to reflect individual harvested trees within site replicates for all models (tree nested in site). The model selection approach applied to branch (Appendix C) and tree-level (Appendix D) predictions used the function *dredge* from the *MuMIn* package to generate a list of all possible model combinations (Barton 2024). The model with the lowest AICc was used, though in certain cases the next best model (within one AIC unit) was employed where model assumptions could not be met with the lowest AICc model. Model assumptions were assessed with diagnostic plots of fitted and residual values and histograms of residuals from the DHARMa package (Hartig 2022). In some instances, models were refitted to allow for unequal variance by fixed-effects factors to better meet model assumptions. Spearman rank correlations were calculated for the observed and model-predicted foliage and live branch biomass.

2.6 Biomass prediction

The approach used for biomass scaling follows that of Schoonmaker et al. (2016) where a subsample of branches was utilized to generate estimates of whole-tree biomass pools using models with high-predictability. These whole tree estimates were then used to generate predictions of biomass pools for all measured trees in the treatment plots based on simpler growth metrics. The general process followed fitting a global model first with subsequent model selection to identify a best-fit model for branch-scale biomass (Appendix C) and then whole-tree biomass (Appendix D).

206 *2.7 Branch-level biomass prediction*

207 The primary branches were divided into length cohorts, which greatly improved the
208 predictability of the fitted biomass prediction models compared to when all sizes of branches
209 were pooled together. These groupings also enabled the use of generalized linear models without
210 data transformation.

211 The following explanatory variables were included in the global models for branch-level
212 biomass prediction: primary branch length categories for small branch biomass (< 30 cm, 30-52
213 cm, 53-76 cm, 77-120 cm, >121 cm), primary branch length as a continuous variable for large
214 branch biomass, relative location of the primary branch within the tree crown from the bottom to
215 the top (0-24%, 25-39%, 40-59%, 60-79%, 80-100%), tree originating from a thinned subplot
216 (yes or no), and primary branch diameter at the base where it intersected with the main stem.
217 Length categories were used where it was important to capture a size gradient, but where the
218 absolute measure of length resulted in poor model fitting or unmet assumptions. For small
219 branch biomass predictions, the 77-120 cm and >121 cm length categories were consolidated
220 into a single group due to insufficient data in the >121 cm category. For large branch biomass
221 predictions, the absolute measure of primary branch length fitted reasonably as a continuous
222 variable.

223 For the small branch component of primary branches < 4 mm in diameter, a median value
224 of 0.5 grams (0.64 mean, range 0.1 to 1.9 grams) was applied because these data did not fit well
225 in the other models and these very small branches contributed only a minor component of the
226 total biomass of the small branch pool. Primary branches with a diameter < 5 mm were assigned
227 zero large branch biomass rather than fitted.

228 Global and fitted models used for prediction of branch-level biomass pools are shown in
229 Table E1 with model coefficients for prediction of foliage, small branch, and large branch
230 biomass are shown in Table E2, E3, and E4, respectively. Branch-level model performance
231 depicted as plots of observed versus predicted biomass are shown in Figures F1 and F2.

232 *2.8 Tree-level prediction of biomass*

233 Once the best-fit branch-level models to predict foliage, small branch, and large branch
234 biomass for each primary branch were determined, these models were then applied to all the
235 measured primary branches in the 52 destructively harvested trees for whole-tree estimates of the
236 different biomass pools. Although dead branches were not sampled for biomass, they were
237 recorded along the main stem and were assigned a large biomass pool only, assuming they had
238 lost all foliage and small branches. The large branch biomass associated with the dead branches
239 was predicted using the living large branch biomass models. The whole-tree biomass pools
240 included foliage mass, small branch mass (< 0.5 cm diameter), and large branch mass (> 0.5 cm
241 diameter, separated into living and dead components).

242 For each biomass pool, these whole-tree estimates were used to fit a global predictive
243 model (y ~ DBH × Live crown percentage × Height) using a model selection approach to
244 determine the best fit model (Appendix D). Live crown percentage refers to the live crown length
245 relative to the total tree height and is generally considered an important predictor of crown
246 biomass (Pulkkinen 1991; Raulier et al. 1996). Model fit and predictability were high for all
247 biomass pools. Model coefficient estimates and model details are shown in table G1.

248 *2.9 Comparison with national equations*

249 The national biomass equations (Ung et al. 2008) using height and DBH were applied to
250 each of the 52 harvested trees to generate biomass predictions of foliage and branch biomass.

These national equations do not include dead biomass. To compare with the total branch biomass from national equations, the small branch biomass and live large branch biomass pools from our locally developed equations were aggregated. For each tree, the predicted foliage and live branch biomass were compared to the observed biomass using both the national equations and our local equations.

In addition, both the national and local equations were used to predict stand-level foliage and branch biomass (kg ha^{-1}) based on the individual tree field measurements from all the lodgepole pine trees within each measurement plot across the nine sites from which we had originally sampled the harvested trees. Generalized linear mixed effect models from the *glmmTMB* package (Brooks et al. 2017) were used to evaluate the effect of the equation (local or national) on foliage from thinned plots, foliage from control plots, branches from thinned plots, and branches from control plots. The gamma distribution with log link function was used for each model. Plot nested within site was included as a random effect for the thinned plot models where each site contained three thinned plots. For the control plots where there was one plot per site, the random effect contained only site.

3. Results

3.1 Tree-level predictions

Fitted models were determined to predict tree-level biomass pools (Table 3). The required parameters for predicting foliage, small branch, and large branch biomass were DBH, height, and live crown percent. Dead large branch biomass prediction required only DBH and live crown percent. The model-derived allometric equations for estimating each biomass pool are

shown in Table 4. The coefficient of determination (R^2) was 0.92 for foliage, small branch, and large branch biomass, and was 0.91 for large dead branch biomass.

Table 3. Global and final models used for prediction of tree-level biomass pools (foliage, small branches < 5 mm diameter, large branches > 5 mm diameter [living vs dead]). LCP = percentage (%) live crown, DBH = diameter at breast height (cm), Height = total tree height (m). All models used a Gamma distribution (log link function) with Site treated as a random effect.

Response variable	Model	Factor levels	Dispersion parameter
Foliage mass	global	DBH × LCP × Height	
	fitted	LCP × DBH + Height × DBH	
Small branch mass	global	DBH × LCP × Height	
	fitted	LCP + Height × DBH	
Large branch - live mass	global	DBH × LCP × Height	DBH × Height
	fitted	LCP × DBH + Height × DBH	
Large branch - dead mass	global	DBH × LCP × Height	
	fitted	LCP × DBH	

Table 4. Model derived equations and marginal R^2 values for predicting whole-tree biomass pools (foliage, small branches < 5 mm, large branches > 5mm [living vs dead]). LCP = percentage (%) live crown, DBH = diameter at breast height (cm), Ht = total tree height (m).

Biomass (g)	Equation	R^2
Foliage	$e^{0.9982 + (0.0425\times LCP) + (0.6734\times DBH) + (0.2099\times Ht) - (0.0029\times LCP\times DBH) - (0.0266\times DBH\times Ht)}$	0.92
Small branches	$e^{2.1684 + (0.3896\times DBH) + (0.1579\times Ht) + (0.0159\times LCP) - (0.0186\times DBH\times Ht)}$	0.92
Large live branches	$e^{-2.1090 + (0.8366\times DBH) + (0.0588\times LCP) + (0.3612\times Ht) - (0.0035\times DBH\times LCP) - (0.0343\times DBH\times Ht)}$	0.92
Large dead branches	$e^{3.7029 - (0.0159\times LCP) + (0.5439\times DBH) - (0.0030\times LCP\times DBH)}$	0.91

285

286 *3.2 Effect of thinning on biomass*

287 Whole-tree biomass estimates were applied to all harvested trees, plotted as a function of
288 DBH, and grouped by treatment (control or thinned) to visualize the effect of thinning on
289 biomass 7-8 years post thinning (Figure 3, a-d). Higher foliage and branch biomass were
290 associated with trees from thinned plots compared to trees from control plots, with larger
291 differences observed at larger DBHs (Figure 3, a-d). The biomass difference between control and
292 thinned plots was more pronounced between live branches compared to when both live and dead
293 branches were included (Figure 3, a-d), illustrating that trees from thinned stands retained more
294 living branches and thus more crown biomass, relative to control trees where crown recession
295 was more pronounced and live crown percent tended to be lower, particularly for trees with
296 larger DBH (Figure 3e). Trees from control plots also tended to be taller than trees from thinned
297 plots of similar DBH (Figure 3f).

298

299

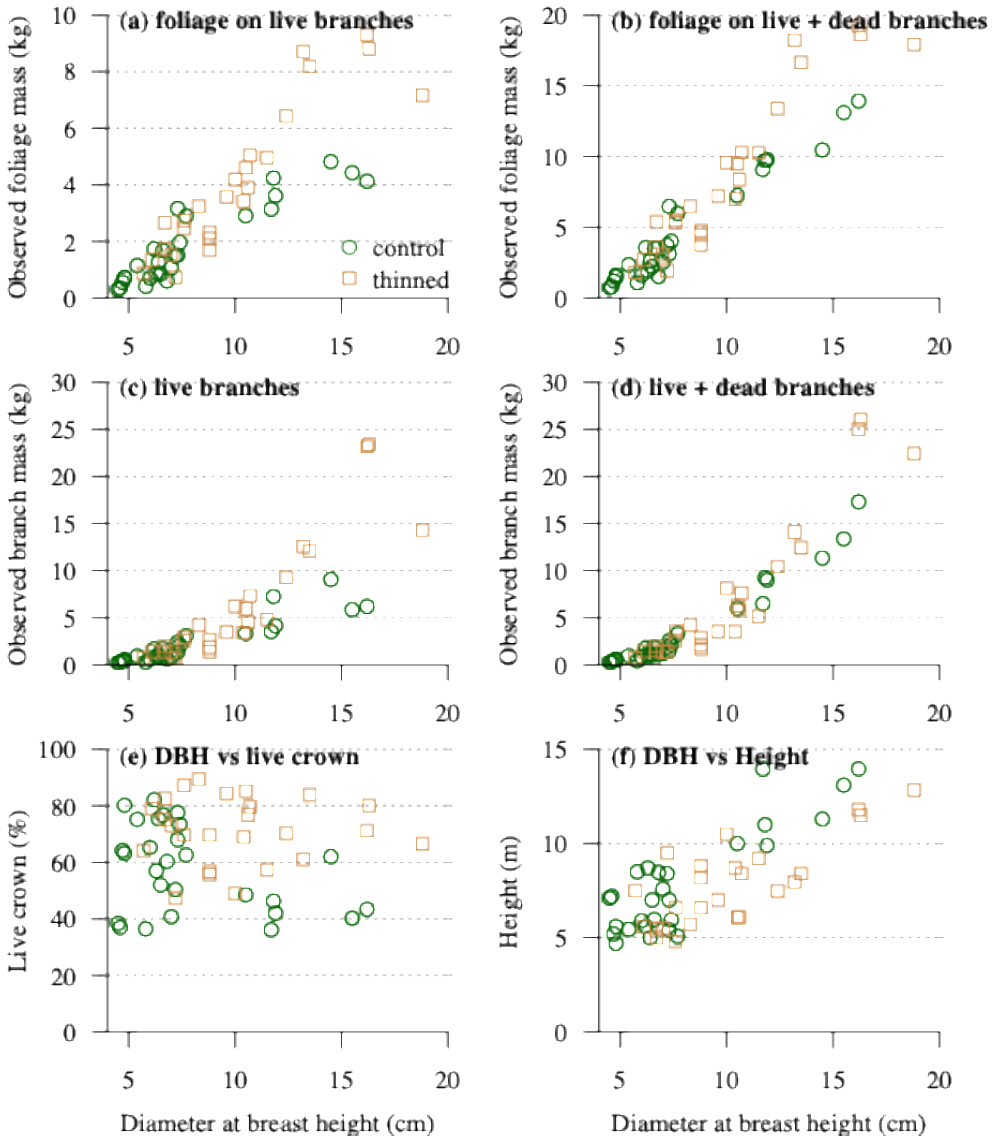


Figure 3. Scatterplots of tree DBH (diameter at breast height) and (a-b) observed foliage, (c-d) live branch mass, (e) live crown percentage and (f) height from control (green circle) and thinned (orange square) plots. Note that for panel (b) the observed foliage reflects an estimate that includes the foliage mass of branches that were dead at the time of harvest and panel (d) includes live + dead branch mass.

3.3 Comparison with national equations

Both our local equations and the national equations were applied to individual trees grouped by treatment (control and thinned) to predict foliage mass and live branch mass. For trees in unmanaged control plots, predicted foliage mass was similar to observed foliage mass using both national and local equations; however, in the thinned plots, national equations tended to underestimate foliage and branch biomass, whereas the local equations tended to slightly overestimate foliage biomass (Figure 4).

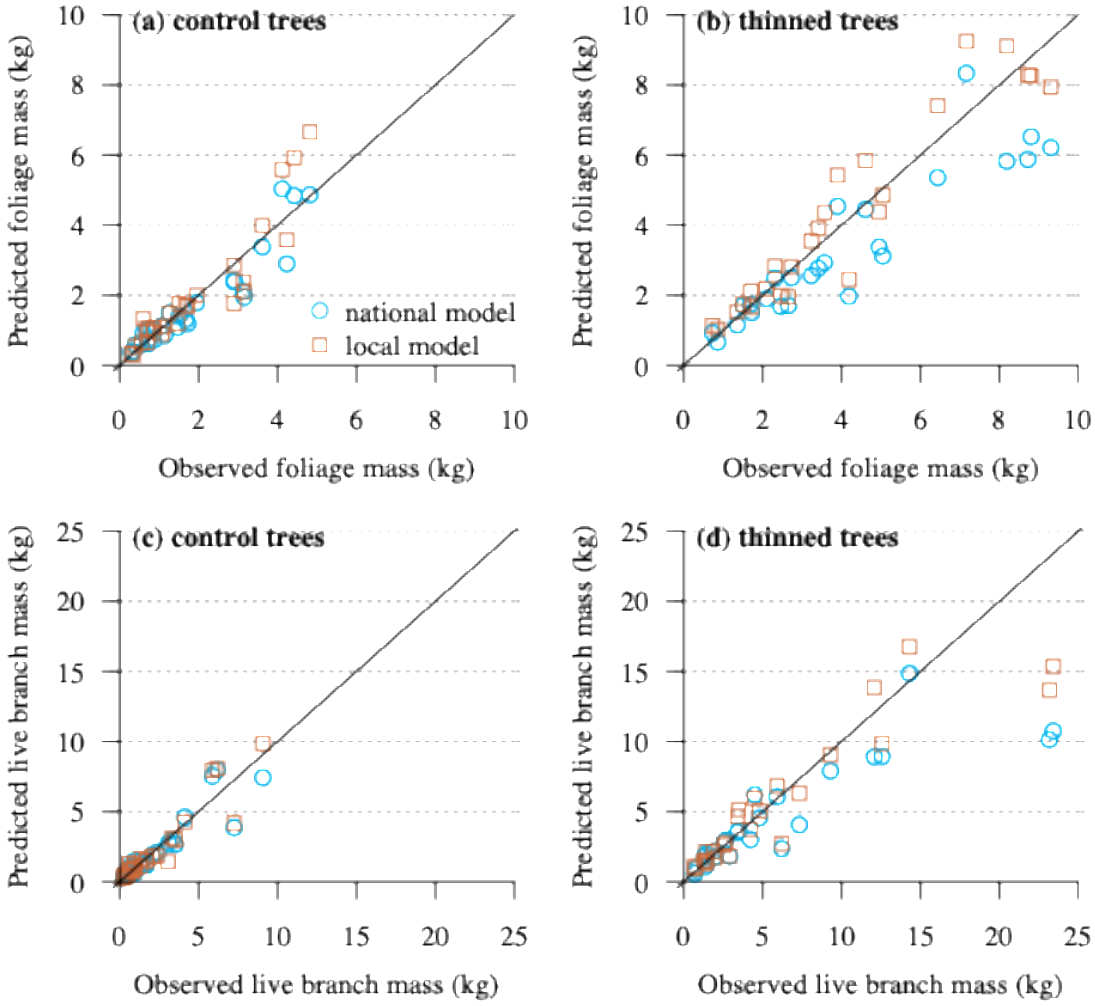


Figure 4. Scatterplots illustrating the relationship between observed and predicted foliage and live branch mass for the national (blue circle) and locally derived (red square) biomass models. The black line reflects a 1:1 relationship. Control trees (a and c) were from plots that were never thinned while thinned trees (b and d) were from plots that had been thinned to various densities 7-8 years prior to harvest.

Both equations were significantly correlated with observed foliage and live branch mass, and the Spearman correlation coefficients (R) and coefficients of determination (R^2) were similar between the two approaches in both control and thinned plots (Table 5). This similarity, however, does not indicate equivalent predictability in managed stands. The two equations diverged as observed foliage mass increased, where the national equations consistently underestimating foliage and live branch mass relative to observed values (Figure 4), a systematic bias not captured by the correlation coefficients.

This underestimation was most apparent when individual tree predictions were scaled up to the stand level (Table 6). In thinned plots, the national equations predicted 14% lower foliage biomass ($P < 0.0001$) and 7% lower branch biomass ($P = 0.004$) than the local equations on average (Table 6), whereas no significant difference was found between equation predictions in the control plots. This result indicated that generalized equations correctly captured crown development in the control plots but failed to capture the enhanced crown development of trees released by pre-commercial thinning.

Table 5. Spearman correlation coefficients and R^2 values for observed vs predicted model estimates of foliage and live branch biomass grouped by thinning treatment.

Response variable	Model compared with observed	Treatment	R	R^2	P-value
Foliage mass	Local	control	0.96	0.91	<0.0001
		thinned	0.94	0.88	<0.0001
	National	control	0.95	0.91	<0.0001
		thinned	0.94	0.89	<0.0001
Live branch mass	Local	control	0.96	0.92	<0.0001
		thinned	0.94	0.89	<0.0001
	National	control	0.95	0.91	<0.0001
		thinned	0.93	0.87	<0.0001

Table 6. Plot-level foliage and branch mass from thinned and control plots predicted using both local and national equations. Values indicate mean with standard error and letters indicate significant differences between equations (α=0.05).

Response variable	Plot-level mass (kg ha^{-1})		
	Local	National	P-value
Foliage from thinned plots	5,694 (702) b	4,879 (602) a	<0.0001
Foliage from control plots	6,951 (808) a	6,751 (785) a	0.3990
Branches from thinned plots	6,493 (1,068) b	6,031 (992) a	0.0042
Branches from control plots	6,895 (994) a	6,929 (998) a	0.9198

4. Discussion

4.1 Predictors of biomass in density managed stands

Our model fitting identified DBH, tree height, and live crown percentage as important predictors of crown biomass pools. These variables were consistently associated with foliage and branch biomass across the density-managed stands examined in this study. Similarly, Lambert et al. (2005) found that DBH was an essential predictor of crown biomass components, although they reported that including height did not substantially improve model accuracy.

The locally developed allometric equations in this study captured the effect of thinning through the incorporation of live crown percentage as a predictor variable. Crown length and live crown attributes are strongly influenced by stand density and competition, making them particularly important for modelling biomass in density-managed stands. Although live crown length is recognized as an important predictor of biomass, it is not always measured in operational inventory plots or forest monitoring programs (Lambert et al. 2005). The results of this study further demonstrate the importance of capturing crown length or related crown metrics when developing biomass prediction equations, particularly in managed stands where crown structure is anticipated to be altered by management practices, such as thinning.

4.2 Effect of thinning on biomass allocation

A significant difference in foliage and branch biomass was observed between the thinned and control plots 7-8 years post treatment for trees of a similar DBH, with increased divergence as DBH increased. Differences between control and thinned stands were more pronounced when only live branch biomass was considered compared with total branch biomass including dead branches. Although trees in the thinned plots had larger live crown lengths, trees in the control plots retained many dead branches, resulting in comparable total branch biomass estimates with

371 thinned plots when the dead branch biomass was included. In addition, dead branch biomass was
372 likely overestimated because reductions in wood density associated with branch mortality was
373 not accounted for.

374 The increased foliage and branch biomass observed on trees from thinned plots relative to
375 trees from control plots of the same DBH has been reported in numerous studies examining the
376 effects of stand density reduction on crown development and biomass allocation (Vanninen et al.
377 1996; Mäkelä and Vanninen 1998). Thinning reduces inter-tree competition for light, water, and
378 nutrients, allowing residual trees to expand their crowns and maintain larger live crown ratios
379 relative to trees growing under dense stand conditions. Increased light availability following
380 thinning can stimulate lateral branch development, foliage retention, and crown depth, resulting
381 in greater allocation of biomass to crown components even among trees of comparable stem
382 diameter (Zeide 2001; Pretzsch 2005). In contrast, trees in the densely stocked control plots of
383 the present investigation typically exhibit reduced crown size and greater self-pruning due to
384 shading and competition, leading to lower branch and foliage biomass.

385 Changes in crown morphology following thinning are particularly important because
386 crown structure is closely linked to photosynthetic capacity and subsequent biomass production.
387 Residual trees in thinned stands often develop wider crowns, larger branch diameters, and longer
388 crown lengths as growing space increases (Pulkkinen 1991; Nilsson and Albrektson 1993;
389 Vincent et al. 2009). Several studies have shown that foliage and branch biomass may increase
390 more rapidly than stem biomass immediately following thinning because crown rebuilding and
391 foliage production are prioritized to maximize light capture and photosynthetic potential
392 (Maguire and Hann 1990; Vanninen and Makela 2000). Over time, increased foliage area can
393 then enhance stem growth and total tree biomass accumulation. When equations are developed

394 from trees within stands that have never received management, reflecting natural rates of self-
395 thinning mortality and associated patterns of crown recession, this may contribute to systematic
396 bias when generalized allometric equations are applied to stands that have received a
397 management treatment, such as pre-commercial thinning.

398 *4.3 Biomass predictions using national equations*

399 Both the locally developed allometric equations and the national allometric equations
400 (Lambert et al. 2005; Ung et al. 2008) detected a significant difference in biomass from thinned
401 versus control stands. Although the national equations did not include the live crown ratio
402 percentage, Lambert et al. (2005) suggested that the height parameter, when combined with
403 DBH, may act as a proxy for the competitive environment experienced by individual trees. The
404 negative height coefficients for lodgepole pine branches and foliage reflects suppressed crown
405 development in trees experiencing competition for light (Lambert et al. 2005; Ung et al. 2008).
406 However, in our data set, the thinned trees tended to be shorter, given the same DBH, relative to
407 control (unthinned trees) and as such, the thinned trees may have experienced a greater
408 penalizing biomass effect, partly explaining why the national model consistently underestimated
409 foliage biomass in the thinned trees but not in the control trees.

410 While the national equations estimated foliage and branch biomass in control stands
411 similarly to local equations, they significantly underestimated foliage and branch biomass in
412 thinned stands by 14% and 7%, respectively compared to the locally developed equations. Their
413 near-identical correlation coefficients (Table 5) do not indicate equivalency in thinned stands.
414 Because the samples collected reflected a continuum of tree sizes, for which both equations
415 perform comparably, correlation and R^2 were largely insensitive to the national equations'
416 underestimation of larger, thinned trees. The stand-level differences in thinned plots (Table 6)

originate from this size-dependent bias rather than loss of correlation. This underestimation of biomass at the stand-scale likely reflects the difficulty of broader-scale equations, developed primarily from natural stands, being able to fully capture how tree crowns respond to reduced stand density after thinning. Particularly for larger, older trees which, under natural circumstances, would be expected to have substantially reduced crown lengths, the development of local equations in managed stands becomes increasingly important.

The underestimation observed in the present study may also reflect local differences in productivity and stand development compared to national averages. As the geographic extent of pooled datasets increases, so does prediction error (Case and Hall 2008). The national equations include trees sampled from Alberta (60 trees), British Columbia (79 trees), and the Yukon (141 trees) (Ung et al. 2008). It is possible that the study area in Alberta was more productive relative to the average conditions represented in the national dataset, allowing biomass predictions in thinned stands to exceed predictions from generalized equations, and biomass predictions in highly competitive control stands to more closely match the national averages. Climate and soil conditions have been shown to significantly influence conifer morphology and biomass accumulation patterns (Gower et al. 1995), which may further contribute to differences between local and national biomass estimates. Furthermore, mixed-effects approaches were not used in the development of national models because of incomplete plot-level information, meaning that stand-level correlation structures within the errors were not accounted for during model fitting as was done with the locally developed equations (Lambert et al. 2005).

It should also be noted that the national biomass equations (Lambert et al. 2005; Ung et al. 2008) include leaf-bearing twigs within the foliage biomass component, whereas the local equations developed in this study separated foliage from twigs and allocated twig mass to the

small branch biomass pool. Consequently, the national equations would be expected to slightly overestimate foliage biomass and underestimate branch biomass relative to the local equations. The observed underestimation of foliage mass from thinned plots using national equations would have been more pronounced had the national equations not included twigs.

Other studies have similarly reported discrepancies between generalized national equations and locally developed biomass models (Case and Hall 2008; Xing et al. 2019; Fradette et al. 2021). With respect to lodgepole pine, Case and Hall (2008) also found that national equations underestimated biomass relative to local equations developed for boreal stands in west-central Canada and relate differences in biomass allometry to both biological and environmental factors. Jenkins et al. (2003) reported that variation among published species-specific biomass regressions often exceeds variation between species themselves, with differences associated with methodology, site-level variability, and relatively small sample sizes used in model development.

These findings suggest that national equations applied to thinned stands may underestimate individual-tree foliage and branch biomass which, when scaled up to the stand level, may have consequences for predicted stand productivity, carbon stocks, and canopy fuel loads. The underestimation of canopy fuel mass is of particular concern from a fire modeling perspective as it translates directly into underestimated canopy bulk density, a critical component for predicting the onset of crowning and crown fire spread (Alexander and Cruz 2014). Locally developed equations or adjustment factors reflecting the effect of forest management practices would improve foliage and branch biomass prediction in density-managed stands. However, to apply a standardized adjustment factor, for PCT for example, additional studies would need to be conducted to capture a broader range of site conditions, geographies and species responses.

4.4 Future studies

Destructive sampling of trees, even relatively young trees, is a laborious task, which is why most authors rely on generalized allometric equations intended for use over larger geographic areas, such as the national equations in Ung et al. (2008). The present investigation has highlighted the risk of this approach when applied to trees and stands that have received density management. Future studies should expand upon our work with other species or within other regions. Further, the apparent size dichotomy (difference between local and national predictions appeared to increase with increased tree size) observed in the present investigation should be further explored. Ultimately, a more generalized understanding of where localized equations are needed and where the national models perform reasonably well would be of value when making future predictions of tree biomass.

With the increased use of remotely sensed data in forest inventories, LiDAR-derived tree metrics provide an effective means of scaling biomass estimation across larger areas while reducing extensive field data collection. Currently, tree detection and segmentation algorithms are used to extract individual tree metrics such as heights and crown diameter from LiDAR point clouds, which are then related to DBH through regressions from forest inventory and applied directly in national allometric equations to estimate biomass (So et al. 2025). However, predictions using these generalized equations relying on multiple regressions, may not be accurate across varying forest conditions, particularly in managed or thinned stands. Future work should focus on developing locally calibrated regression models that relate destructively sampled individual tree biomass to LiDAR-derived tree metrics to provide more accurate biomass predictions in managed forest landscapes, while reducing the cost and time required for traditional inventories (Brede et al. 2022).

5. Conclusions

Density management practices such as PCT altered crown structure and biomass allocation in lodgepole pine stands, resulting in greater foliage and branch biomass relative to trees of comparable size in unmanaged stands. Locally derived allometric equations incorporating live crown attributes improved biomass prediction accuracy and better captured treatment-related differences than national equations, which tended to underestimate foliage and branch biomass in PCT stands. Our findings demonstrated that generalized biomass equations may not adequately represent structural changes associated with silvicultural treatments, particularly where crown morphology differs from the conditions represented in the national dataset. However, we did find consistent agreement between locally derived allometric equations and the national equations when applied to post-harvest stands that were reflective of densities observed in unmanaged, densely stocked lodgepole pine stands, lending further support to the robustness of the national equations being applied to forest stands with limited silvicultural interventions.

Declaration of competing interest: The authors declare that they have no known competing financial interests or personal relationships that could have appeared to influence the work reported in this paper.

Funding: This work was supported by Natural Resources Canada.

Acknowledgements: We would like to acknowledge Jared Salvail, Elizabeth Friel, Kailyn Unka, and Brooke Bourbeau for their assistance in the field and with sample processing.

CRediT authorship contribution statement: Amanda Schoonmaker: Conceptualization, Data curation, Formal analysis, Methodology, Supervision, Writing – original draft, Writing – review and editing. **Angeline Van Dongen**: Formal analysis, Writing – original draft, Writing – review and editing. **Dani Degenhardt:** Funding acquisition, Supervision, Writing – original draft, Writing – review and editing.

Data availability: Data available upon request.

Declaration of generative AI and AI-assisted technologies in the writing process: During the preparation of this work, the authors used Claude to generate the schematic shown in Figure 2. After using this tool, the authors reviewed and edited the content as needed and take full responsibility for the content of the published article.

References

Alexander ME, Cruz MG (2014) Tables for Estimating Canopy Fuel Characteristics from Stand Variables in Four Interior West Conifer Forest Types. For Sci 60:784–794. https://doi.org/10.5849/forsci.13-506

Baah-Acheamfour M, Schoonmaker A, Dewey M, Roth B (2023) Lodgepole Pine and White Spruce Thinning in Alberta—A Review of North American and European Best Practices. Land 12:1261. https://doi.org/10.3390/land12061261

529 Barton K (2024) MuMIn: Multi-model inference

530 Bernier PY, Fournier RA, Ung CH, et al (1999) Linking ecophysiology and forest productivity:
531 An overview of the ECOLEAP project. For Chron 75:417–421.
532 https://doi.org/10.5558/tfc75417-3

533 Bhandari SK, Pinno BD, Stadt KJ, Thomas BR (2024) Growth response to pre-commercial
534 thinning of lodgepole pine is short-term but the effects on size distribution persist for
535 decades. For Chron 100:50–58. https://doi.org/10.5558/tfc2024-002

536 Boudewyn P, Song X, Magnussen S, Gillis MD (2007) Model-based, volume-to-biomass
537 conversion for forested and vegetated land in Canada. Natural Resources Canada
538 Canadian Forest Service Northern Forestry Centre, Victoria, BC

539 Brede B, Terryn L, Barbier N, et al (2022) Non-destructive estimation of individual tree
540 biomass: Allometric models, terrestrial and UAV laser scanning. Remote Sens Environ
541 280:113180. https://doi.org/10.1016/j.rse.2022.113180

542 Brooks M E, Kristensen K, Benthem K J ,van, et al (2017) glmmTMB Balances Speed and
543 Flexibility Among Packages for Zero-inflated Generalized Linear Mixed Modeling. R J
544 9:378. https://doi.org/10.32614/RJ-2017-066

545 Case BS, Hall RJ (2008) Assessing prediction errors of generalized tree biomass and volume
546 equations for the boreal forest region of west-central Canada. Can J For Res 38:878–889.
547 https://doi.org/10.1139/x07-212

548 Fournier RA, Luther JE, Guindon L, et al (2003) Mapping aboveground tree biomass at the stand
549 level from inventory information: test cases in Newfoundland and Quebec. Can J For Res
550 33:1846–1863. https://doi.org/10.1139/x03-099

551 Fradette O, Marty C, Tremblay P, et al (2021) Allometric Equations for Estimating Biomass and
552 Carbon Stocks in Afforested Open Woodlands with Black Spruce and Jack Pine, in the
553 Eastern Canadian Boreal Forest. Forests 12:59. https://doi.org/10.3390/f12010059

554 Gower ST, Isebrands JG, Sheriff DW (1995) Carbon Allocation and Accumulation in Conifers.
555 In: Resource Physiology of Conifers. Elsevier, pp 217–254

556 Gupta SD, Pinno BD, McCready T (2020) Commercial thinning effects on growth, yield and
557 mortality in natural lodgepole pine stands in Alberta. For Chron 96:111–120.
558 https://doi.org/10.5558/tfc2020-016

559 Hall JP, Richardson J (2001) ENFOR - Energy from the forest. For Chron 77:831–835.
560 https://doi.org/10.5558/tfc77831-5

561 Hartig F (2022) DHARMa: Residual Diagnostics for Hierarchical (Multi-Level / Mixed)
562 Regression Models

563 Jenkins JC, Chojnacky DC, Heath LS, Birdsey RA (2003) National-Scale Biomass Estimators
564 for United States Tree Species. For Sci 49:12–35.
565 https://doi.org/10.1093/forestscience/49.1.12

566 Kurz WA, Shaw CH, Boisvenue C, et al (2013) Carbon in Canada's boreal forest — A synthesis.
567 Environ Rev 21:260–292. https://doi.org/10.1139/er-2013-0041

568 Lambert M-C, Ung C-H, Raulier F (2005) Canadian national tree aboveground biomass
569 equations. Can J For Res 35:1996–2018. https://doi.org/10.1139/x05-112

570 Maguire DA, Hann DW (1990) Constructing models for direct prediction of 5-year crown
571 recession in southwestern Oregon Douglas-fir. Can J For Res 20:1044–1052.
572 https://doi.org/10.1139/x90-139

573 Mäkelä A, Vanninen P (1998) Impacts of size and competition on tree form and distribution of
574 aboveground biomass in Scots pine. Can J For Res 28:216–227.
575 https://doi.org/10.1139/x97-199

576 Natural Regions Committee (2006) Natural regions and subregions of Alberta: Natural Regions
577 Committee. Government of Alberta

578 Nilsson U, Albrektson A (1993) Productivity of needles and allocation of growth in young Scots
579 pine trees of different competitive status. For Ecol Manag 62:173–187.
580 https://doi.org/10.1016/0378-1127(93)90049-S

581 Pitt D, Lanteigne L (2008) Long-term outcome of precommercial thinning in northwestern New
582 Brunswick: growth and yield of balsam fir and red spruce. Can J For Res 38:592–610.
583 https://doi.org/10.1139/X07-132

584 Pretzsch H (2005) Diversity and Productivity in Forests: Evidence from Long-Term
585 Experimental Plots. In: Scherer-Lorenzen M, Körner C, Schulze E-D (eds) Forest
586 Diversity and Function. Springer-Verlag, Berlin/Heidelberg, pp 41–64

Pulkkinen P (1991) Crown structure and partitioning of aboveground biomass before the competition phase in a mixed stand of normal-crowned Norway spruce (Picea abies (L.) Karst.) and pendulous Norway spruce (Picea abies f. pendula (Lawson) Sylven). Tree Physiol 8:361–370. https://doi.org/10.1093/treephys/8.4.361

R Core Team (2025) R: A language and environment for statistical computing

Raulier F, Ung C-H, Ouellet D (1996) Influence of social status on crown geometry and volume increment in regular and irregular black spruce stands. Can J For Res 26:1742–1753. https://doi.org/10.1139/x26-198

Reinhardt E, Scott J, Gray K, Keane R (2006) Estimating canopy fuel characteristics in five conifer stands in the western United States using tree and stand measurements. Can J For Res 36:2803–2814. https://doi.org/10.1139/x06-157

Scaria F, Pinno BD (2024) Pre-Commercial Thinning Increases Tree Size and Reduces Western Gall Rust Infections in Lodgepole Pine. Forests 15:808. https://doi.org/10.3390/f15050808

Schoonmaker AS, Lieffers VJ, Landhäusser SM (2016) Viewing forests from below: fine root mass declines relative to leaf area in aging lodgepole pine stands. Oecologia 181:733–747. https://doi.org/10.1007/s00442-016-3621-6

So K, Chau J, Rudd S, et al (2025) Direct Estimation of Forest Aboveground Biomass from UAV LiDAR and RGB Observations in Forest Stands with Various Tree Densities. Remote Sens 17:2091. https://doi.org/10.3390/rs17122091

607 Thiffault E, Hannam KD, Paré D, et al (2011) Effects of forest biomass harvesting on soil
608 productivity in boreal and temperate forests — A review. Environ Rev 19:278–309.
609 https://doi.org/10.1139/a11-009

610 Ung C-H, Bernier P, Guo X-J (2008) Canadian national biomass equations: new parameter
611 estimates that include British Columbia data. Can J For Res 38:1123–1132.
612 https://doi.org/10.1139/X07-224

613 Vanninen P, Makela A (2000) Needle and stem wood production in Scots pine (Pinus sylvestris)
614 trees of different age, size and competitive status. Tree Physiol 20:527–533.
615 https://doi.org/10.1093/treephys/20.8.527

616 Vanninen P, Ylitalo H, Sievänen R, Mäkelä A (1996) Effects of age and site quality on the
617 distribution of biomass in Scots pine (Pinus sylvestris L.). Trees 10:231–238.
618 https://doi.org/10.1007/BF02185674

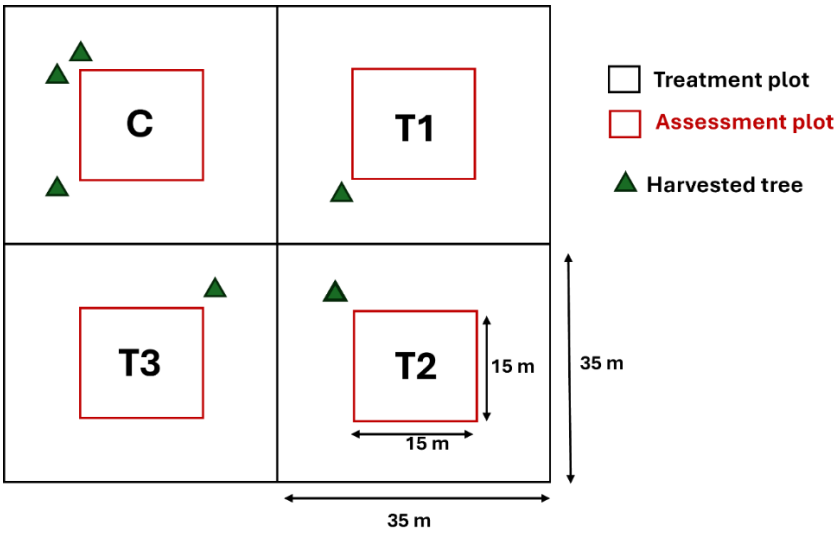
619 Vincent M, Krause C, Zhang SY (2009) Radial growth response of black spruce roots and stems
620 to commercial thinning in the boreal forest. Forestry 82:557–571.
621 https://doi.org/10.1093/forestry/cpp025

622 Xing D, Bergeron JAC, Solarik KA, et al (2019) Challenges in estimating forest biomass: use of
623 allometric equations for three boreal tree species. Can J For Res 49:1613–1622.
624 https://doi.org/10.1139/cjfr-2019-0258

625 Zeide B (2001) Thinning and Growth: A Full Turnaround. J For 99:20–25.
626 https://doi.org/10.1093/jof/99.1.20

APPENDIX A – Site layout and felled tree locations

Figure A1. Site layout showing the assessment plots within treatment plots and locations of felled trees



APPENDIX B – Thinning details

Table B1. Pre-thinning and immediately post-thinning details from each site plot including density, basal area (BA), and percent conifer along with the percent of stems and BA removed from each plot.

Site	Plot	Pre-thinning			Post-thinning			% stems removed	% BA removed
		Density (stems ha^{-1})	BA (m^2 ha^{-1})	% conifer	Density (stems ha^{-1})	BA (m^2 ha^{-1})	% conifer		
210140	C	7,156	23.8	99	7,156	23.8	99	0	0

210140	T1	8,222	28.7	99	1,556	11.0	100	81	62
210140	T2	3,956	15.7	99	2,044	11.2	100	48	29
210140	T3	7,644	31.4	100	2,578	14.5	100	66	54
250206_33	C	8,489	13.4	100	8,489	13.4	100	0	0
250206_33	T1	7,644	15.4	100	1,200	5.5	100	84	65
250206_33	T2	15,911	18.1	99	2,400	5.2	100	85	71
250206_33	T3	5,378	13.8	100	2,622	10.8	100	51	22
250206_50	C	15,333	20.3	100	15,333	20.3	100	0	0
250206_50	T1	13,911	21.2	100	1,378	5.0	100	90	76
250206_50	T2	9,067	16.0	100	2,444	8.1	100	73	49
250206_50	T3	7,467	19.2	100	2,667	10.7	100	64	45

310099	C	4,400	4.3	100	4,400	4.3	100	0	0
310099	T1	6,978	5.9	100	2,178	3.3	100	69	44
310099	T2	5,689	5.9	100	2,356	3.2	100	59	46
310099	T3	6,444	6.5	100	3,467	4.5	100	46	31
502004A	C	4,667	6.0	95	4,667	6.0	95	0	0
502004A	T1	8,222	7.5	95	1,422	3.1	100	83	58
502004A	T2	6,844	6.0	98	2,133	3.4	100	69	44
502004A	T3	7,467	5.8	96	3,111	3.9	100	58	33
502004B	C	7,200	2.5	86	7,200	2.5	86	0	0
502004B	T1	9,156	3.0	85	2,178	1.3	98	76	58
502004B	T2	7,022	1.9	93	2,400	1.0	100	66	45
502004B	T3	8,933	3.5	81	4,889	2.6	99	45	27
690033	C	3,556	25.7	99	3,556	25.7	99	0	0
690033	T1	3,600	28.9	100	1,289	20.4	100	64	29

690145	C	10,933	11.3	41	10,933	11.3	41	0	0
690145	T1	7,511	11.8	90	1,556	5.1	10	79	57
690145	T2	7,911	10.8	90	2,444	5.9	10	69	46
690145	T3	9,956	13.5	97	3,511	8.7	10	65	35
690189	C	5,956	1.1	94	5,956	1.1	94	0	0
690189	T1	4,400	0.7	99	1,156	0.3	10	74	58
690189	T2	5,644	1.2	97	1,422	0.5	10	75	59
690189	T3	6,089	1.0	100	2,578	0.6	10	58	41

Table B2. Site characteristics of sampled locations 7-8 years post thinning including stem density, basal area (BA) and percent conifer.

Site	Plot	Density (stems ha^{-1})	BA (m^2 ha^{-1})	% Conifer
210140	C	9,556	36.3	99
210140	T1	1,600	23.7	100
210140	T2	2,311	22.3	100

210140	T3	2,667	28.3	100
25020633	C	24,000	23.7	100
25020633	T1	1,733	7.8	100
25020633	T2	4,089	10.9	99
25020633	T3	3,733	16.3	100
25020650	C	25,733	30.8	100
25020650	T1	2,667	10.0	100
25020650	T2	3,911	14.9	100
25020650	T3	2,978	17.4	100
310099	C	8,400	24.2	100
310099	T1	2,622	16.1	100
310099	T2	3,200	18.5	100
310099	T3	4,622	19.5	100
502004A	C	10,356	20.7	83
502004A	T1	4,400	10.0	49
502004A	T2	4,889	11.6	62
502004A	T3	4,844	14.3	75
502004B	C	12,889	13.5	81
502004B	T1	5,022	5.4	62
502004B	T2	4,400	5.7	87
502004B	T3	7,733	12.8	83
690033	C	3,911	36.4	81
690033	T1	1,644	33.6	89
690145	C	11,156	23.4	46
690145	T1	2,667	11.5	62
690145	T2	4,489	14.0	80
690145	T3	4,089	18.2	95
690189	C	21,778	16.8	92
690189	T1	6,311	6.6	76
690189	T2	7,111	8.2	51
690189	T3	5,556	11.4	82

APPENDIX C – Model selection approach for branch-scale biomass model development

Model comparison tables are shown illustrating various model fits. As some tables compared many models (multiple interactions possible), only the top 15 models are shown (lowest AIC). Tables were produced using the R package *MuMIn*. The bolded model was selected for final predictions. In some cases, the model with the lowest AIC was not selected due to improved assumptions or model fit statistics associated with a secondary model, typically one that was less than 1 unit of difference in AIC (delta < 1).

Table C1. Summary of models compared for determination of foliage mass for primary branches with diameters < 15 mm in size. Model 24 was selected over model 32 due to better model assumptions (fit). Dmt = branch diameter, Lng_cat = branch length category, Loc_rel_ctg = categorical location of branch within the tree, Thn = thinning treatment (thinned or unthinned) and TDB = tree DBH.

Model ID	cnd((Int))	dsp((Int))	cnd(Dmt)	cnd(Lng_cat)	cnd(Loc_rel_ctg)	cnd(Thn)	cnd(TDB)	df	logLik	AICc	delta
32	-0.2404	+	0.2428	+	+	+	-0.0025	14.0	-2054.6	4137.9	0.0
24	**-0.3100**	**+**	**0.2442**	**+**	**+**		**0.0098**	**13.0**	**-2055.8**	**4138.1**	**0.3**
30	-0.1766	+	0.3447		+	+	-0.0086	11.0	-2125.9	4274.2	136.4
22	-0.2382	+	0.3453		+		0.0034	10.0	-2127.1	4274.5	136.7
4	-0.3880	+	0.2766	+				8.0	-2137.7	4291.6	153.7
12	-0.4002	+	0.2759	+		+		9.0	-2137.5	4293.3	155.4
20	-0.4095	+	0.2764	+			0.0025	9.0	-2137.7	4293.6	155.7

28	-0.4003	+	0.2759	+		+	0.0000	10.0	-2137.5	4295.3	157.5
15	0.7027	+		+	+	+		12.0	-2162.8	4350.1	212.3
31	0.7909	+		+	+	+	-0.0108	13.0	-2162.7	4351.8	214.0
7	0.7946	+		+	+			11.0	-2165.7	4353.8	215.9
23	0.6866	+		+	+		0.0117	12.0	-2165.5	4355.5	217.6
2	-0.2047	+	0.3313					5.0	-2183.9	4377.8	240.0
18	-0.1517	+	0.3322				-0.0064	6.0	-2183.7	4379.4	241.6
26	-0.1398	+	0.3318			+	-0.0109	7.0	-2183.2	4380.5	242.6

658

659

660 **Table C2.** Summary of models compared for determination of foliage mass for branches with
661 diameters > 15 mm in size. Model 22 was selected over model 24 due to better model
662 assumptions (fit). Dmt = branch diameter, Lng_cat = branch length category, Loc_rel_ctg =
663 categorical location of branch within the tree, Thn = thinning treatment (thinned or unthinned)
664 and TDB = tree DBH.

665

Model ID	**cnd((Int))**	**dsp((Int))**	**cnd(Dmt)**	**cnd(Lng_cat)**	**cnd(Loc_rel_ctg)**	**cnd(Thn)**	**cnd(Trh)**	**df**	**logLik**	**AICc**	**delta**
24	4.189	+	0.08931	+	+		-0.09052	11	-990.116	2003.8	0
22	**4.204**	**+**	**0.09262**		**+**		**-0.08741**	**10**	**-991.694**	**2004.7**	**0.89**
32	4.076	+	0.08779	+	+	+	-0.08251	12	-989.657	2005.1	1.37
30	4.088	+	0.09095		+	+	-0.07928	11	-991.206	2005.9	2.18
8	3.45	+	0.08576	+	+			10	-994.499	2010.3	6.5
16	3.373	+	0.08349	+	+	+		11	-993.478	2010.5	6.73
14	3.407	+	0.08576		+	+		10	-995.000	2011.3	7.51
6	3.492	+	0.08846		+			9	-996.209	2011.4	7.69

2	3.213	+	0.06821				5	-1033.546	2077.4	73.67
10	3.177	+	0.06694		+		6	-1033.207	2078.9	75.13
18	3.339	+	0.0697			-0.01602	6	-1033.254	2079	75.22
4	3.222	+	0.06863	+			6	-1033.541	2079.6	75.8
26	3.272	+	0.06825		+	-0.01088	7	-1033.083	2080.8	77.04
12	3.19	+	0.06747	+	+		7	-1033.183	2081	77.24
20	3.352	+	0.07019	+		-0.01618	7	-1033.233	2081.1	77.34

Table C3. Summary of models compared for determination of small branch mass (< 5 mm diameter) for primary branches with diameters 4-14 mm in size. Dmt = branch diameter, Lng_cat = branch length category, Loc_rel_ctg = categorical location of branch within the tree, Thn = thinning treatment (thinned or unthinned) and Trh = tree height.

Model ID	cnd((Int))	**dsp((Int))**	**cnd(Dmt)**	**cnd(Lng_cat)**	**cnd(Loc_rel_ctg)**	**cnd(Trh)**	**df**	**logLik**	**AICc**	**delta**
8	**-0.4701**	**+**	**0.156**	**+**	**+**		**12**	**-1109.986**	**2244.5**	**0**
16	-0.4037	+	0.1561	+	+	-0.008577	13	-1109.62	2245.9	1.36
6	-0.4519	+	0.2077		+		9	-1145.79	2309.9	65.38
14	-0.4463	+	0.2077		+	-0.000727	10	-1145.79	2312	67.45
12	-0.104	+	0.1349	+		-0.02405	9	-1148.713	2315.7	71.23
4	-0.2809	+	0.1328	+			8	-1151.64	2319.5	75.02
7	0.3136	+		+	+		11	-1216.433	2455.3	210.81
15	0.3379	+		+	+	-0.003127	12	-1216.397	2457.3	212.82
10	-0.09055	+	0.2252			-0.02362	6	-1223.959	2460.1	215.55
11	0.4565	+		+		-0.01251	8	-1228.416	2473.1	228.57
13	0.5738	+			+	0.07065	9	-1491.338	3001	756.48
5	1.138	+			+		8	-1497.329	3010.9	766.4

9	1.354	+			0.04331	5	-1568.168	3146.4	901.93

672

673 **Table C4.** Summary of models compared for determination of small branch mass (< 5 mm
674 diameter) for primary branches with diameters 15+ mm in size. Model 12 was selected due to
675 improved model assumptions and prediction. Dmt = branch diameter, Lng_cat = branch length
676 category, Loc_rel_ctg = categorical location of branch within the tree, Thn = thinning treatment
677 (thinned or unthinned) and Trh = tree height.

678

Model ID	cnd((Int))	dsp((Int))	cnd(Dmt)	cnd(Lng_cat)	cnd(Loc_rel_ctg)	cnd(Thn)	cnd(Trh)	df	logLik	AICc	delta
4	1.72	+	0.07304	+				6	-701.657	1415.8	0
12	**1.761**	**+**	**0.07341**	**+**		**+**		**7**	**-701.159**	**1416.9**	**1.16**
8	1.7	+	0.07383	+	+			10	-697.89	1417	1.26
20	1.664	+	0.07276	+			0.006811	7	-701.542	1417.7	1.93
16	1.73	+	0.07414	+	+	+		11	-697.517	1418.6	2.77
24	1.634	+	0.07346	+	+		0.007443	11	-697.756	1419	3.25
28	1.739	+	0.07329	+		+	0.002421	8	-701.145	1419.1	3.32
32	1.692	+	0.0739	+	+	+	0.003927	12	-697.482	1420.8	4.99
6	1.765	+	0.07764		+			9	-709.021	1437.1	21.29
14	1.795	+	0.0781		+	+		10	-708.669	1438.6	22.82
22	1.651	+	0.07705		+		0.01276	10	-708.681	1438.6	22.84
2	1.914	+	0.07786					5	-714.172	1438.7	22.89
10	1.95	+	0.07835			+		6	-713.793	1440.1	24.27
30	1.702	+	0.07751		+	+	0.009637	11	-708.485	1440.5	24.71
18	1.863	+	0.07763				0.006252	6	-714.092	1440.7	24.87

679

Table C5. Summary of models compared for determination of large branch mass (> 5 mm diameter) for primary branches with diameters 1-9 mm in size. Dmt = branch diameter, Lng = branch length, Loc_rel_ctg = categorical location of branch within the tree.

Model ID	cnd((Int))	zi((Int))	dsp((Int))	cnd(Dmt)	cnd(Lng)	cnd(Loc_rel_ctg)	cnd(Dmt:Lng)	zi(Dmt)	zi(Lng)	zi(Dmt:Lng)	df	logLik	AICc	delta
124	**-4.32**	**6.92**	**+**	**0.672**	**0.059**		**-0.0052**	**-0.603**	**0.1309**	**-0.044**	**9**	**-927.2**	**1872**	**0**
60	-4.32	14.4	+	0.672	0.059		-0.0052	-2.09	-0.092		8	-928.9	1874	1.43
128	-4.32	6.92	+	0.676	0.057	+	-0.0051	-0.603	0.1309	-0.044	13	-926.2	1879	6.49
64	-4.32	14.4	+	0.676	0.057	+	-0.0051	-2.095	-0.092		12	-928.0	1880	7.89
116	-1.98	6.92	+	0.367	0.017			-0.603	0.1309	-0.044	8	-937.5	1891	18.6
52	-1.98	14.4	+	0.367	0.017			-2.095	-0.092		7	-939.3	1892	20.0
120	-2.03	6.92	+	0.380	0.016	+		-0.603	0.1309	-0.044	12	-936.2	1897	24.4
56	-2.03	14.4	+	0.380	0.016	+		-2.095	-0.092		11	-938.0	1898	25.8
28	-4.32	13.13	+	0.6766	0.0578	+	-0.005171	-2.523			11	-942.999	1908	35.7
32	-4.32	13.13	+	0.6766	0.0578	+	-0.005171	-2.523			11	-942.999	1908	35.7
20	-1.988	13.12	+	0.3673	0.0178			-2.521			6	-954.271	1920	47.9
24	-2.034	13.13	+	0.3804	0.016	+		-2.523			10	-953.01	1926	53.6

118	-2.089	6.927	+	0.4962	+		-0.603	0.131	-0.0441	11	-953.466	1929	56.6
54	-2.087	14.45	+	0.4959	+		-2.096	-0.092		10	-955.212	1930	58.0
114	-1.841	6.928	+	0.495			-0.603	0.1309	-0.0441	7	-967.954	1950	77.3

684

685

686 **Table C6.** Summary of models compared for determination of large branch mass (> 5 mm
687 diameter) for primary branches with diameters 10-19 mm in size. Dmt = branch diameter, Lng =
688 branch length, Loc_rel_ctg = categorical location of branch within the tree.

689

Model ID	cnd((Int))	dsp((Int))	cnd(Dmt)	cnd(Lng)	cnd(Loc_rel_ctg)	cnd(Dmt:Lng)	df	logLik	AICc	delta
16	**-0.2371**	**+**	**0.2215**	**0.01985**	**+**	**-0.0007322**	**11**	**-828.867**	**1681**	**0**
12	-0.1638	+	0.2277	0.0168		-0.0006749	7	-836.53	1687.6	6.6
8	0.9241	+	0.1401	0.009045	+		10	-833.972	1689	8
4	0.9141	+	0.1512	0.007028			6	-840.681	1693.7	12.77
6	0.9296	+	0.1967		+		9	-866.494	1751.8	70.85
2	1.015	+	0.2003				5	-872.215	1754.7	73.73
7	1.832	+		0.02039	+		9	-916.496	1851.8	170.85
3	1.977	+		0.01655			5	-939.484	1889.2	208.26
5	3.575	+			+		8	-1028.906	2074.5	393.5
1	3.862	+					4	-1036.503	2081.2	400.21

690

691 **Table C7.** Summary of models compared for determination of large branch mass (> 5 mm
692 diameter) for primary branches with diameters 20+ mm in size. Dmt = branch diameter, Lng =
693 branch length, Loc_rel_ctg = categorical location of branch within the tree.

694

Model ID	cnd((Int))	dsp((Int))	cnd(Dmt)	cnd(Lng)	cnd(Loc_rel_ctg)	cnd(Dmt:Lng)	df	logLik	AICc	delta
16	**2.048**	**+**	**0.07369**	**0.0131**	**+**	**-0.0001618**	**11**	**-532.176**	**1089.5**	**0**
8	3.117	+	0.03322	0.008303	+		10	-536.657	1095.9	6.41
12	2.176	+	0.08388	0.01012		-0.0001419	7	-546.693	1108.7	19.16
7	3.386	+		0.01169	+		9	-545.799	1111.7	22.2
4	3.149	+	0.04801	0.006013			6	-549.409	1111.8	22.27
3	3.519	+		0.01031			5	-565.503	1141.7	52.18
2	3.254	+	0.0898				5	-566.887	1144.4	54.95
6	3.059	+	0.08662		+		9	-563.754	1147.6	58.11
5	5.009	+			+		8	-622.97	1263.6	174.1
1	5.529	+					4	-630.016	1268.5	178.98

695

APPENDIX D – Model selection approach for whole tree-scale biomass model development

Model comparison tables are shown illustrating various model fits. Tables were produced using the R package *MuMIn*. The model bold was selected for final predictions.

Table D1. Summary of models compared for determination of whole-tree foliage mass. DBH = diameter at breast height (1.3m), Ht = tree height, LCP = percent live crown.

Model ID	cnd((Int))	dsp((Int))	cnd(DBH)	cnd(Ht)	cnd(LCP)	cnd(DBH:Ht)	cnd(DBH:LCP)	cnd(Ht:LCP)	cnd(DBH:Ht:LCP)	df	logLik	AICc	delta
32	**0.9982**	**+**	**0.6735**	**0.21**	**0.04253**	**-0.02664**	**-0.002976**			**8**	**-399.2**	**817.8**	**0**
128	-2.491	+	0.971	0.6884	0.09804	-0.06449	-0.007493	-0.008003	0.0006079	10	-397.3	819.9	2.1
64	0.8713	+	0.6332	0.2679	0.04504	-0.02631	-0.002322	-0.001096		9	-399	820.2	2.45
48	1.143	+	0.4751	0.3914	0.04368	-0.02417		-0.00364		8	-400.8	820.9	3.13
16	3.147	+	0.428	0.1601	0.01592	-0.02071				7	-406.9	830.2	12.45
12	4.588	+	0.4797	0.0476		-0.02066				6	-412.1	838	20.23
40	3.922	+	0.2669	0.07239	0.03284			-0.002725		7	-411.5	839.6	21.84
24	4.16	+	0.3768	-0.08191	0.02884		-0.001869			7	-411.9	840.4	22.57
22	3.515	+	0.3269		0.03476		-0.001736			6	-413.6	841.1	23.34
6	4.507	+	0.2182		0.01904					5	-415.1	841.6	23.77
8	5.16	+	0.2546	-0.07266	0.01259					6	-413.9	841.6	23.8
56	3.879	+	0.3117	0.0275	0.03349		-0.0007375	-0.001949		8	-411.4	842.2	24.4
4	6.298	+	0.2988	-0.1649						5	-416.8	844.8	27.01
2	5.485	+	0.2437							4	-426	860.9	43.15
7	2.631	+		0.3013	0.04326					5	-441.1	893.5	75.73
39	1.79	+		0.3956	0.05617			-0.00152		6	-440.9	895.7	77.93
5	5.307	+			0.03988					4	-455.9	920.6	102.8
3	6.653	+		0.1583						4	-457.4	923.7	105.9

1	7.945	+							3	-462.7	931.9	114.1

704

705 **Table D2.** Summary of models compared for determination of whole-tree small branch mass.

706 DBH = diameter at breast height (1.3m), Ht = tree height, LCP = percent live crown.

707

Model ID	cnd((Int))	dsp((Int))	cnd(DBH)	cnd(Ht)	cnd(LCP)	cnd(DBH:Ht)	cnd(DBH:LCP)	cnd(Ht:LCP)	cnd(DBH:Ht:LCP)	df	logLik	AICc	delta
16	**2.168**	**+**	**0.389 6**	**0.158**	**0.0159 7**	**- 0.01861**				**7**	**- 335.922**	**688. 4**	**0**
48	1.614	+	0.395 2	0.2221	0.0250 9	- 0.01873		0.001195		8	- 335.147	689. 6	1.25
32	1.723	+	0.440 8	0.164	0.0221 2	- 0.01945	- 0.0006822			8	- 335.369	690. 1	1.7
64	1.603	+	0.402 9	0.2157	0.0250 8	- 0.01884	-0.000113	-0.00106		9	- 335.141	692. 6	4.18
128	- 1.404	+	0.714 2	0.5835	0.0711 2	- 0.05345	-0.004843	- 0.006913	0.000546 5	10	- 333.974	693. 3	4.92
6	3.488	+	0.209		0.0177 4					5	- 344.639	700. 6	12.19
12	3.711	+	0.434	0.02653		- 0.01707				6	- 343.589	701	12.66
8	3.909	+	0.233 2	- 0.04857	0.0137 2					6	- 343.884	701. 6	13.25
40	2.525	+	0.238 2	0.1016	0.0358 1			- 0.002635		7	-342.8	702. 1	13.76
22	3.378	+	0.220 5		0.0194 8		- 0.0001854			6	-344.62	703. 1	14.72
56	2.529	+	0.174 4	0.1722	0.0358 8		0.001065	- 0.003884		8	- 342.329	704	15.62

				-	0.0154		-					704.	
24	3.8	+	0.245	0.04895	9		0.0001895			7	-343.86	3	15.88
			0.284								-	708.	
4	5.111	+	6	-0.1477						5	348.616	5	20.15
			0.242									721.	
2	4.31	+	1							4	-356.19	2	32.84
					0.0428						-	758.	
7	1.482	+		0.298	8					5	373.604	5	70.12
					0.0403						-	761.	
39	1.646	+		0.2797	5			0.000296		6	373.595	1	72.67
					0.0442						-	787.	
5	3.82	+			5					4	389.213	3	98.89
											-	797.	108.9
3	5.231	+		0.1861						4	394.257	4	7
											-	807.	118.7
1	6.752	+								3	400.315	1	4

Table D3. Summary of models compared for determination of whole-tree live large branch mass. DBH = diameter at breast height (1.3 m), Ht = tree height, LCP = percent live crown.

Model ID	cnd((Int))	dsp((Int))	cnd(DBH)	cnd(Ht)	cnd(LCP)	cnd(DBH:Ht)	cnd(DBH:LCP)	cnd(Ht:LCP)	cnd(DBH:Ht:LCP)	df	logLik	AICc	delta
32	**-2.1**	**+**	**0.84**	**0.36**	**0.06**	**-0**	**-0**			**8**	**-400**	**820**	**0**
128	-7	+	1.37	0.93	0.13	-0.1	-0	-0	0	10	-399	822	2.76
64	-2	+	0.86	0.33	0.06	-0	-0	0		9	-400	823	2.86
48	-1.5	+	0.59	0.53	0.06	-0		-0		8	-403	825	5.23
16	0.27	+	0.58	0.34	0.03	-0				7	-406	828	7.87
22	1.3	+	0.5		0.05		-0			6	-411	837	16.9
6	3.03	+	0.32		0.02					5	-413	838	18.1
40	0.17	+	0.33	0.32	0.07			-0		7	-411	838	18.6

24	1.2	+	0.5	0.01	0.05		-0			7	-411	839	19.5
12	2.6	+	0.66	0.15		-0				6	-413	840	19.9
8	3.01	+	0.32	0	0.02					6	-413	840	20.7
56	-0	+	0.41	0.24	0.07		-0	-0		8	-411	841	20.8
4	5.07	+	0.4	-0.2						5	-418	848	27.9
2	4.29	+	0.34							4	-422	853	33.1
7	-0.3	+		0.48	0.06					5	-438	887	67.1
39	-1.3	+		0.6	0.08			-0		6	-438	889	69.4
5	3.79	+			0.06					4	-456	920	100
1	7.86	+								3	-465	937	117

712

713 **Table D4.** Summary of models compared for determination of whole-tree dead large branch

714 mass. DBH = diameter at breast height (1.3m), Ht = tree height, LCP = percent live crown.

715

Model ID	cnd((Int))	dsp((Int))	cnd(DBH)	cnd(Ht)	cnd(LCP)	cnd(DBH:Ht)	cnd(DBH:LCP)	cnd(Ht:LCP)	cnd(DBH:Ht:LC	df	logLik	AICc	delta
6	**5.75**	**+**	**0.35**		**-0**					**5**	**-352**	**715**	**0**
22	3.7	+	0.54		-0		-0			6	-351	716	0.98
8	4.51	+	0.28	0.14	-0					6	-351	716	1.28
24	1.84	+	0.5	0.17	0		-0			7	-350	716	1.62
16	3.1	+	0.42	0.3	-0	-0				7	-350	717	2.6
32	0.41	+	0.65	0.34	0	-0	-0			8	-349	718	2.79
40	2.81	+	0.28	0.33	-0			-0		7	-351	718	3.27
56	2.28	+	0.56	0.05	-0		-0	0		8	-350	719	4.25
64	0.98	+	0.9	0.07	-0	-0	-0	0.01		9	-349	719	4.53
48	1.96	+	0.41	0.43	-0	-0		-0		8	-350	720	4.98
4	1.41	+	0.16	0.38						5	-355	721	6.62
128	-4.2	+	1.38	0.72	0.07	-0.1	-0	-0	0	10	-348	722	6.89
12	-0.3	+	0.33	0.59		-0				6	-354	722	7.39
3	1.32	+		0.58						4	-359	728	12.9
7	1.49	+		0.57	-0					5	-359	730	15.3

39	0.18	+		0.72	0.02		-0	6	-359	732	17.6
2	3.68	+	0.25					4	-362	733	17.9
1	6.07	+						3	-374	755	39.8
5	6.11	+			-0			4	-374	757	42.2

716

717

APPENDIX E – Models for branch-level biomass predictions

Table E1. Global and final models used for prediction of branch-level biomass pools (foliage, small branches < 5 mm diameter, large branches > 5 mm diameter) by primary branch size class based on diameter at stem intersection. Diam = primary branch diameter at base, LengthC = categorical grouping variable for primary branch length, Length = continuous measure of primary branch length, LocC = relative location of the primary branch along the main stem, Treatment = whether the tree was in an unthinned or thinned treatment area, Tree DBH = diameter at breast height (cm), Tree ht = total tree height (m). All models used a Gamma distribution (log link function) with Site and Tree within Site treated as random effects.

Response variable	Primary branch diameter (mm)	Model type	Fixed effects	Dispersion parameter
Foliage mass	< 15	global	Diam + LengthC + Tree DBH + LocC + Treatment	
		fitted	Diam + LengthC + Tree DBH + LocC	Diam × LocC
	15 +	global	Diam + LengthC + Tree Ht + LocC + Treatment	
		fitted	Diam + Tree Ht + LocC	Diam × LocC
Small branch mass	4 - 14	global	Diam + LengthC + Tree Ht + LocC + Treatment	
		fitted	Diam + LengthC + LocC	LocC
	15 +	global	Diam + LengthC + Tree Ht + LocC + Treatment	
		fitted	Diam + LengthC + LocC	Diam
	6-9	global	Diam × Length + LocC	Diam × Length

Large branch mass		fitted	Diam × Length	Diam × Length
	10 - 19	global	Diam × Length + LocC	
		fitted	Diam × Length + LocC	
	20+	global	Diam × Length + LocC	
		fitted	Diam × Length + LocC	

728

729

730 **Table E2.** Model coefficients for branch-level prediction of foliage mass for primary branches <
731 15 mm or 15+ mm base diameter at the intersection from the main stem. Diameter = branch
732 diameter at intersection with main stem, Length_cat = categorical grouping variable for branch
733 length (L1= < 30 cm, L2 = 30-52 cm, L3 = 53-76 cm, L4 = 77-120 cm and L5 = 121+ cm),
734 Loc_rel_cat = relative location of the branch along the main stem, Tree DBH = diameter at
735 breast height (cm), Tree height = total tree height (m).

736

Group	**Parameter**	**Estimate**	**Standard error**	**z-value**	**p-value**
Branch base diameter <15 mm	(Intercept)	-0.1033	0.1452	-0.712	0.4770
	Diameter	0.2283	0.0133	17.119	<0.0001
	Length_catL2	0.8499	0.0738	11.51	<0.0001
	Length_catL3	1.2481	0.0917	13.618	<0.0001
	Length_catL4	1.2839	0.1277	10.051	<0.0001
	Tree DBH	-0.0035	0.0121	-0.287	0.7740
	Loc_rel_catC25	-1.5576	0.1469	-10.606	<0.0001
	Loc_rel_catC40	-0.7569	0.0918	-8.245	<0.0001

	Loc_rel_catC60	-0.4281	0.0767	-5.583	<0.0001
	Loc_rel_catC80	-0.0319	0.0544	-0.586	0.5580
Branch base diameter 15+ mm	(Intercept)	3.7903	0.2111	17.955	<0.0001
	Diameter	0.0847	0.0075	11.254	< 2e-16
	Tree height	-0.0440	0.0173	-2.546	0.0109
	Loc_rel_catC25	-1.5144	0.2200	-6.884	<0.0001
	Loc_rel_catC40	-1.0225	0.1968	-5.197	<0.0001
	Loc_rel_catC60	-0.5417	0.1358	-3.988	0.0001
	Loc_rel_catC80	-0.1882	0.1082	-1.739	0.0819

Table E3. Model coefficients for branch-level prediction of small branch (< 5 cm) mass for primary branches < 15 mm or 15+ mm in diameter at the intersection from the main stem. Diameter = branch diameter at intersection with main stem, Length_cat = categorical grouping variable for branch length (L1= < 30 cm, L2 = 30-52 cm, L3 = 53-76 cm, L4 = 77-120 cm and L5 = 121+ cm), Loc_rel_cat = relative location of the branch along the main stem.

Group	Parameter	Estimate	Standard error	z-value	p-value
Branch base diameter 4-14 mm	(Intercept)	-0.4856	0.0734	-6.617	<0.0001
	Diameter	0.1598	0.0098	16.232	<0.0001
	Length_catL2	0.4228	0.0584	7.239	<0.0001
	Length_catL3	0.4934	0.0686	7.195	<0.0001
	Length_catL4	0.7184	0.0930	7.726	<0.0001
	Loc_rel_cat25	0.4788	0.0659	7.262	<0.0001
	Loc_rel_cat40	0.4538	0.0491	9.234	<0.0001
	Loc_rel_cat60	0.3210	0.0481	6.673	<0.0001
	Loc_rel_cat80	0.2109	0.0451	4.677	<0.0001

Branch base diameter 15+ mm	(Intercept)	1.6793	0.1071	15.677	<0.0001
	Diameter	0.0754	0.0044	17.299	<0.0001
	Length_catL5	0.3634	0.0701	5.185	<0.0001
	Loc_rel_cat25	-0.1492	0.1026	-1.454	0.1460
	Loc_rel_cat40	-0.0457	0.1007	-0.454	0.6500
	Loc_rel_cat60	0.0445	0.0883	0.503	0.6150
	Loc_rel_cat80	-0.0057	0.0857	-0.067	0.9470

744

745

746 **Table E4.** Model coefficients for branch-level prediction of large branch (> 5 cm) mass for
747 primary branches 6-9 mm, 10-19 mm or 20+ mm in diameter at the intersection from the main
748 stem. Length = continuous measure of total branch length (cm), Diameter = branch diameter at
749 intersection with main stem, Loc_rel_cat = relative location of the branch along the main stem.

750

Group	**Parameter**	**Estimate**	**Standard error**	**z-value**	**p-value**
Primary branch diameter 6-9 mm	(Intercept)	-4.3222	0.5150	-8.392	<0.0001
	Length	0.0590	0.0090	6.573	<0.0001
	Diameter	0.6721	0.0691	9.721	<0.0001
	Diameter × Length	-0.0052	0.0011	-4.762	<0.0001
Primary branch diameter 10-19 mm	(Intercept)	-0.2371	0.3689	-0.643	0.5204
	Length	0.0199	0.0035	5.717	<0.0001
	Diameter	0.2215	0.0266	8.327	<0.0001
	Loc_rel_cat25	-0.1786	0.0819	-2.18	0.0293
	Loc_rel_cat 40	-0.2071	0.0630	-3.289	0.0010
	Loc_rel_cat 60	-0.1038	0.0541	-1.919	0.0550
	Loc_rel_cat 80	-0.0311	0.0487	-0.639	0.5227

	Diameter × Length	-0.0007	0.0002	-3.256	0.0011
Primary branch diameter 20+ mm	(Intercept)	2.0484	0.3739	5.478	<0.0001
	Length	0.0131	0.0018	7.345	<0.0001
	Diameter	0.0737	0.0150	4.913	<0.0001
	Loc_rel_cat 25	-0.3918	0.1251	-3.131	0.0017
	Loc_rel_cat 40	-0.2001	0.1214	-1.649	0.0992
	Loc_rel_cat 60	-0.0402	0.1139	-0.353	0.7239
	Loc_rel_cat 80	-0.0004	0.1036	-0.004	0.9971
	Diameter × Length	-0.0002	0.0001	-3.094	0.0020

751

752

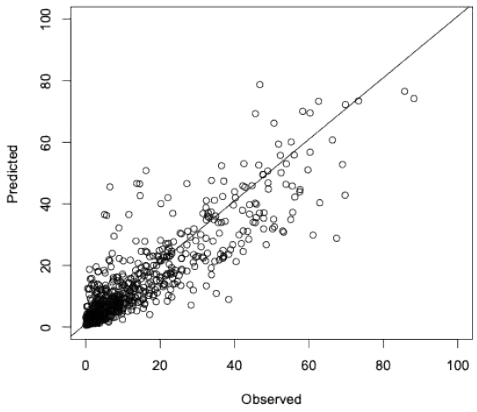
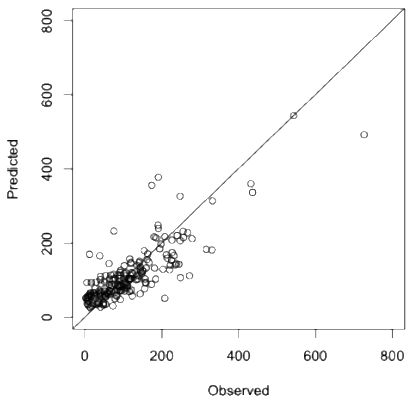
753

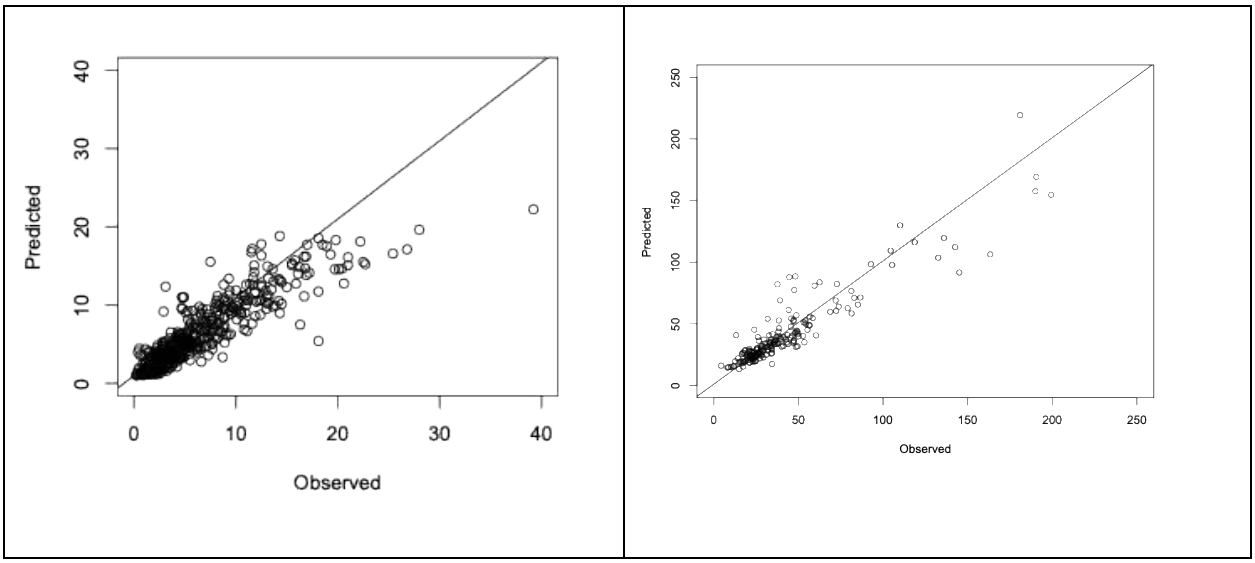
754 **APPENDIX F – Branch-level model performance and prediction**

755

756 **Figure F1.** Observed vs predicted values for foliage mass for primary branches < 15 mm and
757 primary branches > 15 mm diameter at the intersection with the main stem and small branch (< 5
758 mm diameter) mass for primary branches <15 mm, and 20+ mm diameter at the intersection with
759 the main stem.

760

Foliage mass for primary branches < 15 mm diameter	**Foliage mass** for primary branches > 15 mm diameter
	
Small branch mass for primary branches 4-14 mm in diameter	**Small branch mass** for primary branches 4-14 mm in diameter



761

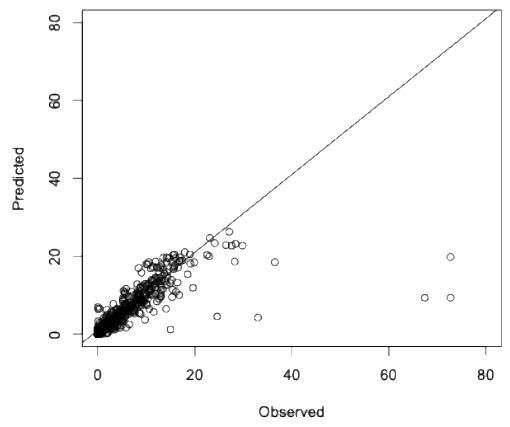
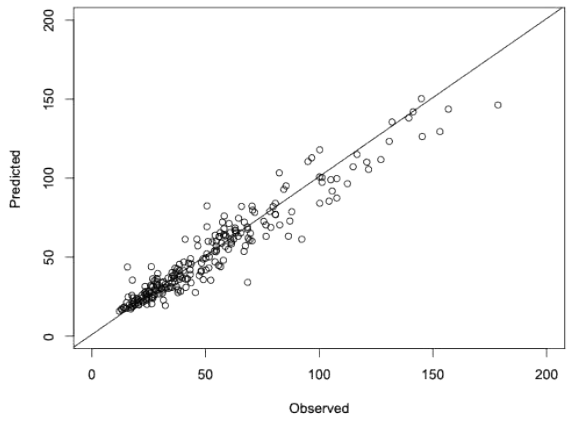
762

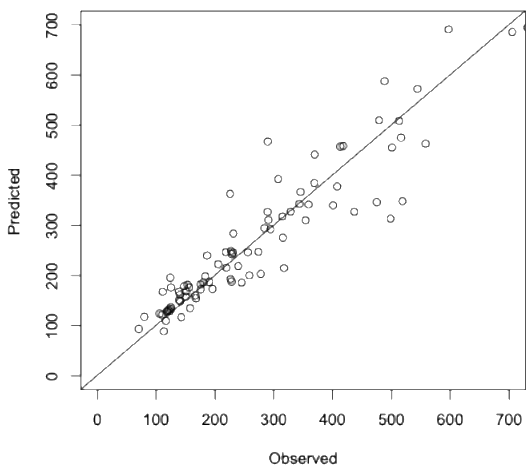
763 **Figure F2.** Observed vs predicted values for large branch (> 5 mm diameter) mass models for

764 primary branches 6-9 mm, 10-19mm, and 20+ mm diameter at the intersection with the main

765 stem.

766

Large branch mass for branches 6-9 mm diameter	**Large branch mass** for branches 10-19 mm diameter
	

Large branch mass for branches 20+ mm in diameter	
	

767

APPENDIX G: Model coefficient estimates for tree-level biomass predictions

Table G1. Model coefficients for predicting whole-tree biomass pools (foliage, small branches < 5 mm, large branches > 5mm [living vs dead]). LCP = percentage (%) live crown, DBH = diameter at breast height (cm), Height = total tree height (m). Marginal R^2 values are also included under the response column for each fitted model.

Response variable	Parameter	Estimate	Standard error	z-value	p-value
Whole tree foliage	(Intercept)	0.9982	0.733	1.362	<0.0001
	LCP	0.0425	0.007	5.872	<0.0001
	DBH	0.6734	0.071	9.538	<0.0001
$R^2 = 0.92$	Height	0.2099	0.062	3.412	<0.0001
	LCP × DBH	-0.0029	0.001	-4.293	<0.0001
	DBH × Height	-0.0266	0.005	-5.866	<0.0001
Whole tree - small	(Intercept)	2.1684	0.524	4.137	<0.0001
branches	DBH	0.3896	0.042	9.286	<0.0001
$R^2 = 0.92$	Height	0.1579	0.058	2.705	<0.0001
	LCP	0.0159	0.004	4.249	<0.0001
	DBH × Height	-0.0186	0.004	-4.259	<0.0001
Whole tree - large live	(Intercept)	-2.1090	0.991	-2.129	0.0332
branches	DBH	0.8366	0.096	8.738	<0.0001
	LCP	0.0588	0.011	5.437	<0.0001
$R^2 = 0.92$	Height	0.3612	0.084	4.301	<0.0001
	DBH × LCP	-0.0035	0.001	-3.5	0.0004
	DBH × Height	-0.0343	0.006	-5.387	<0.0001
	(Intercept)	3.7029	3.882	0.954	<0.0001

Whole tree - large dead branches	LCP	-0.0159	0.061	-0.261	0.7940
$R^2 = 0.81$	DBH	0.5439	0.351	1.549	0.1210
	LCP × DBH	-0.0030	0.006	-0.552	<0.0001

774